Chemical Science

RSC Publishing

EDGE ARTICLE

View Article Online
View Journal | View Issue

Cite this: *Chem. Sci.*, 2013, **4**, 2028

Rapid and selective *spiro*-cyclisations of *O*-centred radicals onto aromatic acceptors†

Roy T. McBurney,‡*[a] Annika Eisenschmidt,[b] Alexandra M. Z. Slawin[b] and John C. Walton*[b]

Received 21st February 2013
Accepted 14th March 2013

DOI: 10.1039/c3sc50500f

www.rsc.org/chemicalscience

Substituted benzyloxycarbonyloxyl radicals were generated by sensitised photolyses of benzyl oxime carbonates. EPR spectroscopy showed they ring closed exclusively by *spiro*-cyclisation onto the *ipso*-C-atoms of the aromatic rings. β-Scission of the alkoxycarbonyloxyls to CO_2 and benzyloxyl radicals increasingly competed and became dominant above 270 K. The first rate parameters for *spiro*-cyclisations of *O*-centred radicals onto aromatics were obtained by the steady-state kinetic EPR method. Pentafluoro-substitution of the ring substantially reduced the *spiro*-cyclisation rate. Activation barriers of the *spiro*-cyclisations were computed by DFT to be about half those of the alternative *ortho*-cyclisations. Consideration of the TS structures suggested the preference for *spiro*- over *ortho*-cyclisation resulted from better overlap of the oxyl SOMO with the aromatic π-system during *spiro* closure.

1 Introduction

Ring closures onto aromatic rings by free radicals necessarily involve disruption of the 6π-electron system. For aryl species with 4-member radical arms **1** the two main options are: (i) *ipso*-attack (Ar_1-5 closure) with formation of a *spiro*-cyclohexadienyl intermediate **2**, or (ii) *ortho*-attack (Ar_1-6 closure) with formation of a bicyclo-cyclohexadienyl intermediate **4** (Scheme 1). *Spiro*-cyclisations involve formation of strained quaternary C-atoms and have no straightforward reaction channel for return to aromaticity. They can be reversible, depending on the architecture of the chain and the extent of strain in the *spiro*-radical. Furthermore, if the chain is unsymmetrical as in **2**, then ring-opening may occur in the alternative mode to generate radical **3**. This amounts to a 1,4-aryl group migration. On the other hand *ortho*-cyclisations can easily be followed by return to aromaticity either by transfer out of the labile H-atom, or by transfer of an electron to a suitable sink with generation of the corresponding carbo-cation, followed by proton loss.

Not surprisingly therefore, most reported ring closures onto aromatics are of the second *ortho*-type. In the great majority of such processes the radical is *C*-centred; often an aryl radical as in the Pschorr and related reactions.[1]

Spiro-centres are important structural motifs in many natural products and pharmaceuticals,[2] so considerable effort has gone into developing radical-based *spiro*-cyclisations.[3,4] Aromatics[5] and hetero-aromatics[6] were found to be suitable radical *spiro*-acceptors. Kinetic or other data to help predict the efficiency of a novel aromatic ring closure, or to help decide which mode would be favoured, is very sparse. Rate constants were estimated for cyclisations of 4-phenylbutyl[7] and 4-naphthylbutyl[8] and the *spiro*-cyclisation of the latter was shown to be reversible at 350 K by deuterium scrambling experiments.[8,9] However, other evidence indicated these rate constants were probably over-estimates.[10] The paucity of information is even more marked for *spiro*-cyclisations of *O*-centred radicals for which *spiro*-intermediates have only been suggested in a few instances with aroyloxyls.[11]

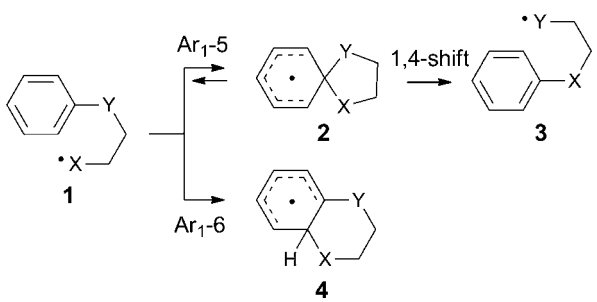

Scheme 1 Ring closure options for radicals with 4-member arms onto aromatic rings.

[a]*University of St. Andrews, EaStCHEM School of Chemistry, St. Andrews, Fife, KY16 9ST, UK*

[b]*University of St. Andrews, EaStCHEM School of Chemistry, St. Andrews, Fife, KY16 9ST, UK. E-mail: jcw@st-and.ac.uk; Fax: +44 (0)1334 463808; Tel: +44 (0)1334 463864*

† Electronic supplementary information (ESI) available: General procedures: preparation and characterization data of oxime carbonates. Sample EPR spectra and kinetic data. X-ray structural data for **6d**, **6f**, **6g** and **7a**. ^{1}H and ^{13}C NMR spectra for novel compounds. DFT computed GS and TS structures. CCDC 923531–923534. For ESI and crystallographic data in CIF or other electronic format, see DOI: 10.1039/c3sc50500f

‡ Current address: School of Chemistry, University of Glasgow, Glasgow G12 8QQ, UK. E-mail: roy.mcburney@glasgow.ac.uk.

We discovered recently that oxime carbonates ArC(R)=N–OC(O)OR′ are clean and convenient precursors for iminyl and *O*-centered radicals.[12] Their weak N–O bonds selectively cleave on UV photolysis, particularly when sensitized with 4-methoxyacetophenone (MAP), thus facilitating investigations of the behavior of both iminyl ArC(R)=N· and alkoxycarbonyloxyl radicals R′OC(O)O·. A distinct advantage of these precursors is that they enable the iminyl radical intermediates to be directly monitored by EPR spectroscopy. Although alkoxycarbonyloxyl radicals are EPR silent,[12,13] the radicals derived from them can be characterized by EPR, thus providing mechanistic insight into the evolution of their chemistry. We have now prepared a set of model oxime carbonates with the aim of studying competition between Ar_1-5 and Ar_1-6 ring closures of the released radicals and of obtaining kinetic information. The test collection was built around a functionalized benzyloxy core linked to either a benzaldehyde or an acetophenone oxime (Scheme 2). In **6a–d** and **7a**,**b** appropriate substituents modified the aromatic character of the benzyl unit. In **6f–i** potential radical leaving groups were incorporated into the benzyl 4-substituents. The precursors with R^1 = H were particularly valuable for EPR spectroscopy because the PhC(H)=N· radicals released on photolysis have very large (~80 G) hyperfine splittings (hfs) from their iminyl H-atoms. Thus the signals from this iminyl are situated in the wings of the EPR spectrum where they do not obscure other radicals but provide a valuable reference. This paper reports our study of the chemistry of *O*-centred alkoxycarbonyloxyl radicals by means of solution EPR spectroscopy, product analyses and DFT computations. This enabled us to obtain the first kinetic data for *spiro*-cyclisations of *O*-centred radicals. The results allowed us to place *spiro*-cyclisations in context with cyclisations in general and to assess the viability of this reaction channel in relation to others.

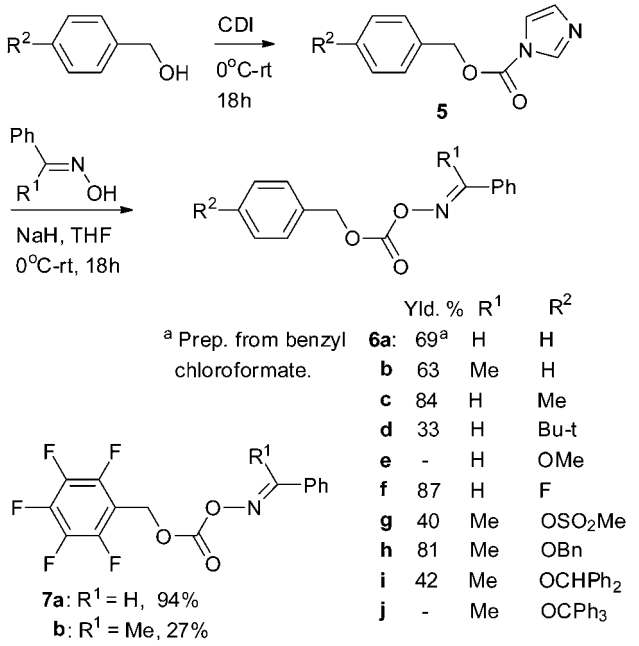

[a] Prep. from benzyl chloroformate.

	Yld. %	R^1	R^2
6a	69[a]	H	H
b	63	Me	H
c	84	H	Me
d	33	H	Bu-t
e	-	H	OMe
f	87	H	F
g	40	Me	OSO_2Me
h	81	Me	OBn
i	42	Me	$OCHPh_2$
j	-	Me	$OCPh_3$

Scheme 2 Benzyloxy oxime carbonates studied.

2 Results and discussion

Preparation of precursor oxime carbonates

For the benzyloxy oxime carbonates **6** we employed our new synthetic method, which avoids lab use of phosgene, and is useful when the chloroformate of the alcohol is not commercially available.[12b] The requisite alcohols were reacted with carbonyldiimidazole to afford intermediates of type **5**. Reaction of these with an oxime and sodium hydride then afforded the oxime carbonates in satisfactory yields (Scheme 2).

Oxime carbonates **6d**,**f**,**g** and **7a** were obtained in crystalline form and the X-ray crystallographic structure of **6f** is shown in Fig. 1.[14] The iminyl OC(O)O units adopted extended *all trans* conformations with nearly planar ArC(R)N–OC(O)O sections. These near planar structures will promote π–π stacking of the oxime moieties with the MAP photosensitizer and hence facilitate energy transfer. The N–O bond lengths [1.441(3), 1.472(7), 1.434(8) and 1.47(1) Å in **6d**, **6f**, **6g** and **7a** respectively] were comparable to that of the analogous bond of an oxime oxalate amide (1.453 Å),[15] and of dioxime oxalates (1.442 Å).[16] Both these classes of compound undergo N–O bond scission on UV irradiation, so similar behavior for **6** and **7** was expected.

Ring closures of alkoxycarbonyloxyl radicals

The photolytic reactions of oxime carbonates **6a–d**,**f–i** and **7a**,**b** were investigated in solution by 9 GHz EPR spectroscopy. Deaerated samples of each oxime carbonate, plus 1 equiv. of MAP, in *t*-BuPh or cyclopropane solvent, were irradiated with unfiltered UV light from a medium pressure Hg lamp directly in the spectrometer resonant cavity. The spectrum obtained from **6c** (Fig. 2a) showed an overlapping mixture of PhC(H)=N· [*g*-factor = 2.0030, *a*(1N) = 9.8, *a*(1H) = 80.1 G; similar to those reported][17] and a second cyclohexadienyl type radical. Similar spectra, consisting of an iminyl radical and a cyclohexadienyl radical, were obtained from the oxime carbonates **6a–d**,**f–i** in the temperature range 210 to 290 K. EPR parameters are in Table 1 and the spectrum from **6f** is also shown in Fig. 2b.

Photo-dissociations of **6** were expected to lead to iminyl radicals (**Im**) together with alkoxycarbonyloxyls **8** (see Scheme 3). The EPR parameters (Table 1) demonstrated unambiguously that the cyclohexadienyl radicals generated from **6** were the corresponding 1,3-dioxaspiro[4,5]decadien-2-onyls **9** and *not* the dihydro-4*H*-benzo[1,3]dioxin-2-onyls **11**. The DFT computed EPR hfs of the radicals (Table 1) provided supporting evidence. It follows that type **8** phenalkoxycarbonyloxyl

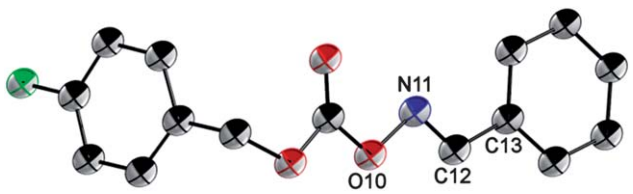

Fig. 1 X-Ray crystal structure of benzaldehyde *O*-4-fluorobenzyloxycarbonyl oxime **6f**. [Selected bond lengths and dihedral angles: O10–N11, 1.472(7) Å, O10–N11–C12–C13 −178.63(46)°.]

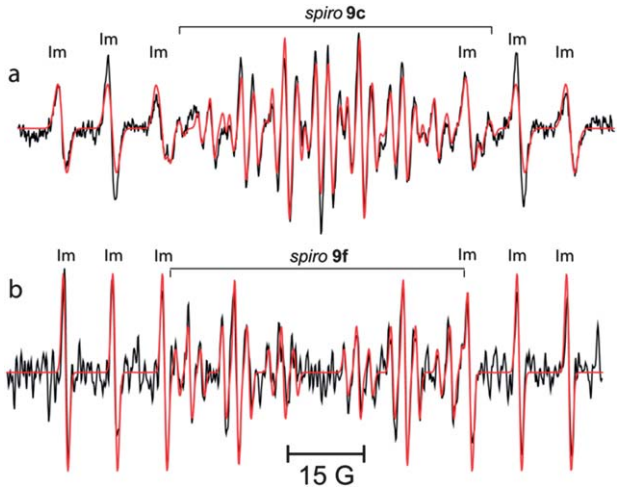

Fig. 2 EPR spectra during photolyses of benzyloxy oxime carbonates. (a) 4-Methyl precursor **6c** at 215 K in *t*-BuPh showing **Im** and **9c**. (b) 4-Fluoro-precursor **6f** at 200 K in cyclopropane showing **Im** and **9f**. Experimental spectra in black and simulations in red.

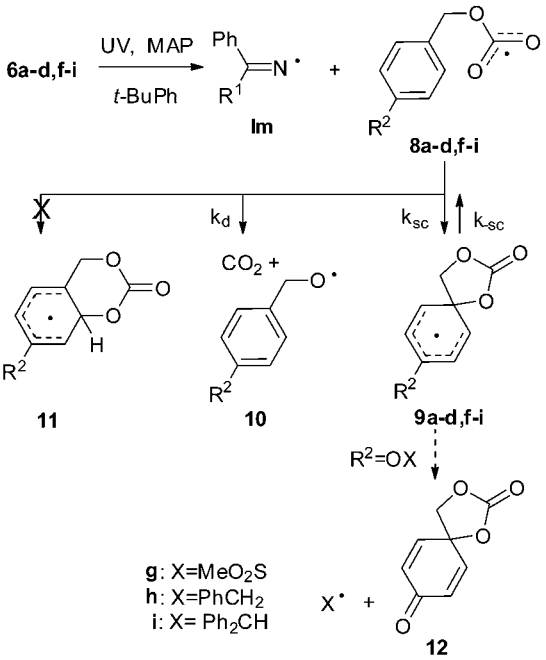

Scheme 3 Ring closures and dissociations of benzyloxycarbonyloxyl radicals.

radicals ring closed selectively in *spiro*-mode (5-*exo*) onto the *ipso* C(1) atoms of their aromatic rings.

The concentration ratios [**9**]/[**Im**] were determined from the EPR spectra obtained from oxime carbonates **6c**,**d**. The data was rather scattered, because of the low *S*/*N*, but in each case [**9**]/[**Im**] was ~1.0 at $T = 220$ K and dropped to near zero by 290 K. The best quality data was obtained with the 4-*t*-Bu-precursor **6d** and is shown in Fig. 3. Photolyses of precursors **6** will yield equal amounts of **Im** and **8** so the observation that [**9**]/[**Im**] = 1.0 indicated that *spiro*-cyclisations of **8c**,**d** were very rapid at $T < 220$ K.

The reduction in [**9**]/[**Im**] to higher temperatures can be accounted for by increasing competition from dissociation of **8** to benzyloxyl radicals **10** and CO_2. No new radicals were detected at higher temperatures in the spectra from **6c**,**d**, as expected with this decarboxylation process, because alkoxyls **10** are known to be EPR "silent". No radicals $ArOC(O)OCH_2^{\cdot}$ were detected from any of the precursors at any temperature. It follows that rearrangements by 1,4-Ar migrations with production of radicals of type **3** did not compete.

The data from precursor **6c** was of lower quality but the drop off in signal from *spiro*-radical **9c** occurred in the same temperature window. This is the same temperature region as was previously observed for the unsubstituted radicals from **6a**,**b**. We conclude that the rate parameters for CO_2 loss from $ArCH_2OC(O)O^{\cdot}$ are about the same for H, Me and *t*-Bu substituents in the 4-position. This is in accord with expectation because 4-substituents are comparatively remote from the breaking O–C(O) bond and separated from it by an sp^3 C-atom.

The main products from UV photolyses of **6a–d**,**f** with MAP at rt were shown by ^{1}H NMR and GC-MS analyses to be the corresponding benzyl alcohols $R^2C_6H_4CH_2OH$, dimer **Im**$_2$, **Im**H and the corresponding aldehyde or ketone from **Im**H hydrolysis. In the case of the benzaldehyde-derived oximes **6a** and **6c**,**d**,**f**, nitriles $R^2C_6H_4CN$ were also obtained *via* the electrocyclic CO_2 loss process described previously.[12] At rt the EPR data showed loss of CO_2 predominates and the observation of

Table 1 Experimental and computed EPR hfs for 1,3-dioxaspiro[4,5]-decadien-2-onyl radicals **9**[a]

Precursor	Radical (R^2)	Temp.[b]/K or DFT	*g*-Factor	$a(H^{2,6})$	$a(H^{3,5})$	$a(R^4)$	$a(H^{\gamma})$
6a	**9a** (H)	230	2.0023	9.0	2.7	13.0(1H)	0.6(2H)
6a	**9a** (H)	DFT	—	−9.4	3.4	−13.5(1H)	−0.8(2H)
6c	**9c** (Me)	205	2.0020	8.7	2.3	14.6(3H)	—
6d	**9d** (*t*-Bu)	215	2.0023	8.6	2.5	—	0.8(1H)
6e	**9e** (OMe)	DFT	—	−9.1	3.1	−0.5(3H)	−0.8(2H)
6f	**9f** (F)	230	2.0025	9.0	2.6	32.8(1F)	—
6f	**9f** (F)	DFT	—	−9.4	3.2	24.1(1F)	−0.8, −0.1
6h	**9h** (OCH2Ph)	230	2.0026	8.2	2.0	2.0(2H)	—
6h	**9h** (OCH2Ph)	DFT	—	−8.5	2.4	2.9(2H)	−0.8, −0.3
6i	**9i** (OCHPh2)	235	2.0026	8.2	2.1	1.3(1H)	—
6i	**9i** (OCHPh2)	DFT	—	−8.5	2.4	1.2(1H)	−0.6, −0.1

[a] In *t*-BuPh solution; hfs in Gauss. [b] DFT with the UB3LYP/6-311+G(2d,p) method; note that the signs of hfs cannot be obtained from isotropic EPR spectra.

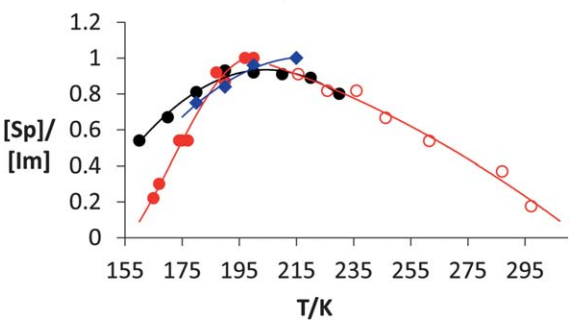

Fig. 3 Variation in relative yields [**spiro**]/[**Im**] with temperature. Black circles: data for unsubstituted **6a** in cyclopropane. Red circles: data for 4-*t*-Bu compound **6d** (filled in cyclopropane, open in *t*-BuPh). Blue diamonds: data for 4-F compound **6f**.

$R^2C_6H_4CH_2OH$, $R^2C_6H_4CN$, and the iminyl-derived products, is in good accord with this.

The pentafluoro-precursors **7a,b** gave rise to significantly different behaviour. Sensitized photolyses of **7a** (and **7b**) in *t*-BuPh yielded spectra showing the corresponding iminyl radical and a second species with EPR parameters as follows: g = 2.0026, a(1H) = 33.5, a(1H) = 13.1, a(1H) = 9.3, a(1H) = 8.1, a(1H) = 2.7 G at 210 K (Fig. 4a and b). We attribute this spectrum to the *meta*-adduct radical from addition of the $C_6F_5CH_2OC(O)O^{\cdot}$ radical (**8F5**) to the *t*-BuPh solvent. The [adduct]/[**Im**] ratio was found to be 0.9 at 225 K showing that virtually all the $C_6F_5CH_2OC(O)O^{\cdot}$ radicals added to solvent. Hence *spiro*-cyclisation of **8F5** must have been significantly slower than this intermolecular addition and slower than for radicals **8a–d,f–i**.

EPR spectra from MAP sensitized photolyses of **7a** in cyclopropane solvent in the temperature range 150–235 K showed

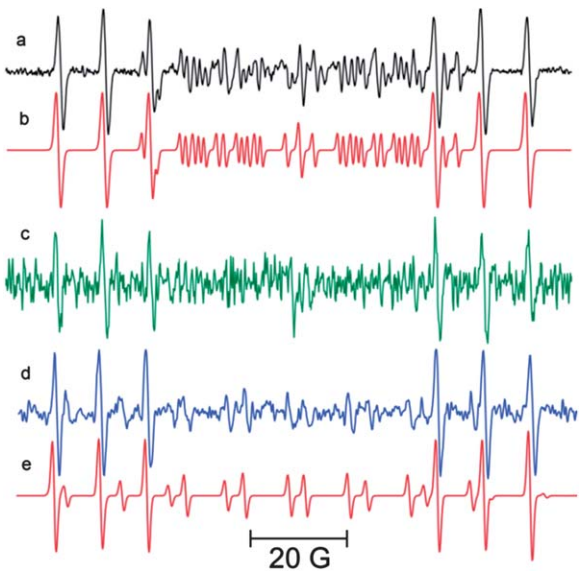

Fig. 4 EPR spectra from UV photolyses of pentafluoro-precursor **7a** in different solvents. (a) UV photolysis of **7a** in *t*-BuPh at 225 K showing **Im** and **8F5** radicals. (b) Simulation of (a). (c) UV photolysis of **7a** in cyclopropane at 155 K showing only **Im**. (d) UV photolysis of **7a** in *n*-pentane at 290 K. (e) Simulation of (d) including **Im**, pent-2-yl and pent-3-yl radicals.

only the iminyl PhCH=N˙ [see Fig. 4(c)]. It follows that *spiro*-cyclisation of $C_6F_5CH_2OC(O)O^{\cdot}$ was slower than termination reactions in this temperature range. The EPR spectrum obtained from irradiation of **7a** in *n*-pentane at 290 K showed a mixture of **Im** (53%), pent-2-yl (25%) and pent-3-yl (22%) [Fig. 4(d) and (e)]. It follows that H-abstraction from the *n*-pentane was more rapid than *spiro*-cyclisation.[18] We infer that the *spiro*-cyclisation of alkoxycarbonyloxyl radicals onto C_6F_5 was materially slower than onto phenyl itself or to phenyl with electron-releasing substituents.

The slower ring closure rate of **8F5** suggested to us that the cyclisations of the other alkoxycarbonyloxyls might be observable by EPR spectroscopy at lower temperatures. Accordingly photolyses of precursors **6a,d** and **f** were examined in cyclopropane solvent and the [**spiro**]/[**Im**] ratios are plotted in Fig. 3.[19] We interpret the curved [**spiro**]/[**Im**] plots as follows. In the temperature range 160–200 K, where [**spiro**]/[**Im**] increased, *spiro*-cyclisation increased in importance converting more **8** to **9** until at about 200 K where [**9**] reached parity with [**Im**]. Above this temperature CO_2 loss from **8** supervened and hence the [**9**]/[**Im**] ratio passed through a maximum and then declined.

The mechanism *before the onset of decarboxylation* (<200 K) will be as shown in Scheme 3, with the addition of self-termination and cross-termination processes for **Im**, **8** and **9** radicals. Making the steady-state approximation it can easily be shown that:[20]

$$k_{sc}/2k_t = [\mathbf{9}]/[\mathbf{8}] \times \{k_{-sc}/2k_t + [\mathbf{8}] + [\mathbf{9}] + [\mathbf{Im}]\} \quad (1)$$

where all the terminations were assumed to be diffusion controlled and have the same rate constant $2k_t$, and k_{-sc} is the rate constant for reverse ring-opening of the *spiro*-radicals **9**. Equi-molar quantities of **Im** and **8** will be formed in the initial photochemical bond fission and hence [**Im**] = [**8**] + [**9**]. Thus eqn (1) can be written as:

$$k_{sc}/2k_t = [\mathbf{9}]/\{[\mathbf{Im}] - [\mathbf{9}]\} \times \{k_{-sc}/2k_t + 2[\mathbf{Im}]\} \quad (2)$$

In principle the concentration [**Im**] could be varied, for example by altering the intensity of UV irradiation, and the corresponding [**9**] determined by EPR. Then both $k_{sc}/2k_t$ and $k_{-sc}/2k_t$ could be obtained by appropriate solution of eqn (2). In practice the S/N in the EPR experiments was too small to allow application of this method. If the reverse ring-opening of *spiro*-radicals **9** is significantly slower than cyclisation then: $k_{-sc}/2k_t \ll 2[\mathbf{Im}]$ and eqn (1) simplifies to:

$$k_{sc}/2k_t = 2[\mathbf{9}][\mathbf{Im}]/\{[\mathbf{Im}] - [\mathbf{9}]\} \quad (3)$$

Rate constants k_{sc} were derived for the unsubstituted, 4-*t*-Bu- and 4-fluoro-radicals **8a,c** and **f** by use of eqn (3) with the radical concentrations determined from the EPR measurements in the T < 200 K region. Since all the radicals are small, terminations will be diffusion controlled, so the well-established $2k_t$ rate parameters for *t*-Bu˙ radicals derived by Fischer and Schuh[21] [log A_t = 11.63 M^{-1} s^{-1}, E_t = 2.25 kcal mol^{-1}], corrected for changes in solvent viscosity as described previously,[22] were used for $2k_t$ without introducing serious errors. Fig. 5 shows the resulting Arrhenius plots.

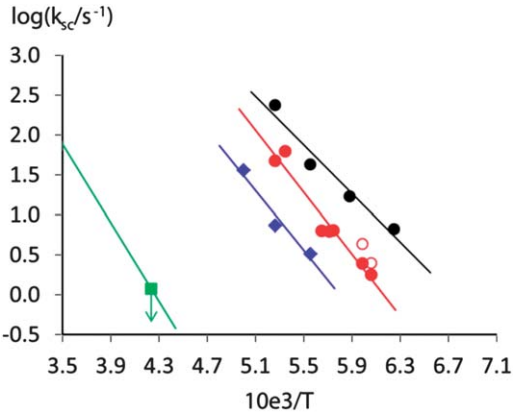

Fig. 5 Arrhenius plots of *spiro*-cyclisation rate data for benzyloxycarbonyloxyls. Black circles for unsubstituted radical **8a**; red circles for 4-*t*-Bu-radical **8d**; red open circles for **8d** calculated with eqn (4) including reverse ring opening; blue diamonds for 4-F-radical **8f**; green square: estimate for penta-F-radical **8F5** from precursor **7a**.

The logarithms of the pre-exponential factors derived from linear regression of the Arrhenius plots of k_{sc} for the three radicals **8a**, **8d** and **8f** were 10.3 ± 1.3, 12.0 ± 1.1 and 10.8 ± 1.8. These are in the expected range for radical cyclisations in solution. However, the temperature range was too short and the data too scattered for these to be reliable. Most radical cyclisations have $\log(A_c/s^{-1})$ close to 10.5,[23] so, for consistency in comparing the data, this value was assumed for all the *spiro*-cyclisation data in Table 2. From the absence of any detectable *spiro*-radical in the spectrum from the pentafluoro-precursor **7a** at 235 K we estimate that [**spiro**]/[**Im**] < 0.2 and hence, utilizing the measured [**Im**] in the analogue of eqn (3), k_{sc} for $C_6F_5CH_2OC(O)O^{\cdot}$ (**8F5**) was estimated to be <0.8 s^{-1} at 235 K. By assuming $\log(A_{sc}/s^{-1}) = 10.5$ for **8F5** the limiting rate data listed in Table 2 was derived and is included in Fig. 5.

These are the first measurements of rate data for *spiro*-cyclisations onto aromatic rings by *O*-centred radicals. In fact, published kinetic data for *spiro*-cyclisations (or *ortho*-cyclisations even of *C*-centred radicals onto aromatic rings) is extremely sparse (Table 2). A note of caution needs to be sounded in that the *spiro*-cyclisation of 4-naphthylbutyl was shown to be reversible at about 350 K by deuterium scrambling experiments.[7,8] If the *spiro*-cyclisations of benzyloxycarbonyloxyls **8** were also appreciably reversible the measured k_{sc} values would be subject to error.

In the special case of the rate constants for *spiro*-cyclisation and reverse ring opening being equal then eqn (2) simplifies to (4):

$$k_{sc}/2k_t = 2[\mathbf{9}][\mathbf{Im}]/\{[\mathbf{Im}] - 2[\mathbf{9}]\} \quad (4)$$

In fact for all the data, except the two lowest temperature points for **8d**, we found that 2[**9**] > [**Im**] so that eqn (4) leads to impossible k_{sc} rate constants. This indicates that k_{-sc} is probably smaller than k_{sc} in the *T* range of the EPR experiments. The two low temperature points for **8d**, calculated from (4), are shown in Fig. 5 and do not deviate greatly from the line obtained by neglecting reverse ring opening. The EPR experiments were carried out at about 100 K lower than the deuterium scrambling study with 4-naphthylbutyl. This also militates against participation by reverse *spiro*-ring opening in our system. We conclude that k_{-sc} must be significantly less than k_{sc} for all **8** and that the rate data in Table 2 is reasonably reliable.

Table 2 Rate data for 5-*exo*- and *spiro*-cyclisations of *C*- and *O*-centered radicals

Radical	Mode	$\log(A_c^a/s^{-1})$	E_c/kcal mol^{-1}	k_c (300 K)/s^{-1}	Ref.
	5-*Exo*	10.4	6.85	2.3×10^5	23
	5-*Exo*	[10.5]	~5.2	~5×10^6	12b
	*Spiro*			<5×10^4 (323 K)	7 and 10
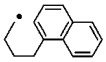	*Spiro*			<10^4 (353 K)	8 and 10
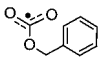	*Spiro*	[10.5]	7.2 ± 1.1	2×10^5	This work
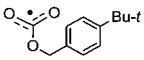	*Spiro*	[10.5]	7.7 ± 0.9	8×10^4	This work
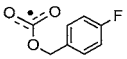	*Spiro*	[10.5]	8.3 ± 2.1	3×10^4	This work
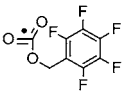	*Spiro*	[10.5]	>11.3	<0.2×10^3	This work

[a] Values in parenthesis assumed.

The data in Table 2 demonstrate that the rate constant for the archetype **8a** is nearly an order of magnitude greater than the estimated rate constants for *spiro*-cyclisations of the *C*-centred analogues 4-phenylbutyl[7] and 4-naphthylbutyl.[8] The faster rate of *spiro*-cyclisation of benzyloxycarbonyloxyl **8a** is as expected by analogy with the larger rate constant for 5-*exo*-cyclisation of allyloxycarbonyloxyl in comparison with hex-5-enyl[9b] (see Table 2). Similarly, alkoxycarbonyloxyl radicals add to alkenes more rapidly than do *C*-centred radicals.[13,24] The data showed that the E_{sc} and k_{sc} values for *spiro*-cyclisation of **8d** with the 4-*t*-Bu substituent differed little from those of unsubstituted **8a**. The EPR observations with precursor **6c** having a 4-Me substituent suggested radical **8c** underwent *spiro*-cyclisation at least as fast as **8a**. The 4-fluoro substituent had a small inhibitory effect on *spiro*-cyclisation but five fluorine substituents reduced the rate and increased the activation energy significantly.

Compounds **6g–j** were prepared to test the idea that the *spiro*-radicals **8g–j** might dissociate to release a new radical **X**$^{\cdot}$ with formation of 1,3-dioxaspiro[4,5]deca-6,9-diene-2,8-dione **12** (Scheme 3). This had potential to be a preparatively useful process. EPR spectra from the sulfonate ester **6g** showed only the corresponding iminyl (**Im**) and iminoxyl PhC(Me)NO$^{\cdot}$ in the range 225 to 285 K. No $MeSO_2^{\cdot}$ radicals were detected.[25]

The benzyloxy-(**6h**) and diphenylmethyloxy-precursors (**6i**) gave good spectra of the corresponding *spiro*-radicals **9h** and **9i** at 220 K (EPR parameters in Table 1) together with **Im**. The *spiro*-radical spectra of **9i** and **9j** weakened to ~280 K and above this only **Im** was detectable; neither the benzyl nor the diphenylmethyl radical appeared. The EPR data suggested that the alkoxycarbonyloxyls **8h,i** dissociated to **10h,i** and CO_2 at these higher temperatures thus precluding *spiro*-cyclisation followed by dissociation to **12** and **X**. GC-MS analysis of the products from photolysis of **6i** supported this conclusion. The major products were found to be 4-$BnOC_6H_4CHO$, 4-$BnOC_6H_4CH_2OH$ and $\mathbf{Im}_2$ from CO_2 loss and termination reactions of **10i** and **Im**. Precursor **6j**, which might have released the much more persistent $Ph_3C^{\cdot}$ radical, was unstable and could not be obtained pure.

QM computations

To shed further light on the competition between *spiro*- and *ortho*-cyclisation for the benzyloxycarbonyloxyl radicals **8**, QM computations were carried out with several methods.[26] Our first task was to test some levels of theory using the experimental data for cyclisation of **8a** as the benchmark. As mentioned before (Table 2), the *spiro*-cyclisation of **8a** exhibited a value for E_{sc} of 7.2 ± 1.1 kcal mol^{-1}, assuming $\log(A_{sc}/s^{-1}) = 10.5$. We therefore took this value as a good approximation of the real value and used it to validate our theoretical approach. Full details are given in the ESI.† Becke's 3-parameter hybrid exchange potential (B3) with the Perdew–Wang (PW91)[27] gradient-corrected correlation functional, UB3PW91, and the 6-311+G(2d,p) basis set was deemed to be unsatisfactory because it gave $\Delta E^{\ddagger}_{298}$ values for *spiro*-cyclisations *decreasing* as one and then five F-atoms were introduced to the ring; contrary to experiment. The Møller–Plesset perturbation theory MP2 method, with a 6-311+G(2d,p) basis set and geometries derived from UB3LYP/6-311+G(2d,p) computations, was also discounted because the $\Delta E^{\ddagger}_{298}$ values for *spiro*-cyclisations greatly exceeded experiment (18.2 kcal mol^{-1} for **8a** and 17.5 kcal mol^{-1} for **8f**). M06 hybrid meta functionals were reported to have broad applicability and M06-2X was found to be good for main group elements.[28] However, $\Delta E^{\ddagger}_{298}$ values computed for *spiro*-cyclisations with M06-2X (also with UB3LYP/6-311+G(2d,p) geometries) were much too small (2.9 for **8a** and 2.2 for **8f**). Our best results were obtained with the standard B3LYP functional and the 6-311+(2d,p) or the correlation consistent polarized triple zeta cc-pvtz basis sets (Table 3). For the series of radicals **8a,c–f** and **8F5** (the pentafluoro-analogue) both the *spiro*- and the *endo*-ring closure processes were explored and the transition structures leading to the five- and six-membered species were computed. The derived activation parameters [$\Delta E^{\ddagger}_{298}$] and reaction enthalpies [ΔH_{298}], corrected to 298 K for thermal effects are listed in Table 3.

For all six benzyloxycarbonyloxyls, **8a,c–f** and **8F5**, the computed $\Delta E^{\ddagger}_{298}$ values were smaller (by nearly a factor of two) for *spiro*- than for *ortho*-cyclisation. Thus, irrespective of substituents, *spiro*-cyclisation was predicted to be favoured in agreement with experiment. The *spiro*-cyclisation reaction enthalpies (ΔH_{298}) for the archetype **8a** and **8c–e** radicals indicate small exothermicities. Slight endothermicities were found for the F-substituted radicals **8f** and **8F5**. This implies that reverse *spiro*-ring opening reactions might be important and is somewhat at odds with experiment (see above). The computed $\Delta E^{\ddagger}_{298}$ values for *spiro*-cyclisations show a decreasing trend from the electron-withdrawing to the electron-releasing substituents. The absolute magnitudes of the computed $\Delta E^{\ddagger}_{298}$ values were all smaller than found by experiment (Table 3). The B3LYP functional is known to underestimate barrier heights[29] (on average by about 4 kcal mol^{-1}) so our results conform with this same tendency.

Table 3 DFT computed activation energies ($\Delta E^{\ddagger}_{298}$) and reaction enthalpies (ΔH_{298}) in kcal mol^{-1} for benzyloxycarbonyloxyl radicals with the UB3LYP functional

Subs.		*Spiro*	*Spiro*	*Ortho*	*Ortho*	*Spiro*
Struct.	Method[a]	$\Delta E^{\ddagger}_{298}$	ΔH_{298}	$\Delta E^{\ddagger}_{298}$	ΔH_{298}	$E^{\ddagger}_{sc}$ expt.
F_5 **8F5**	A	7.70	0.59	13.72	−2.13	>11.2
F_5 **8F5**	B	7.74	0.72	13.58	−2.25	>11.2
4-F **8f**	A	5.38	0.38	12.65	6.35	8.3
4-F **8f**	B	5.83	0.16	13.02	6.45	8.3
8a	A	5.89	−0.45	12.01	5.74	7.2
8a	B	6.35	−0.03	12.35	5.74	7.2
4-Me **8c**	A	4.96	−0.6	12.0	−1.0	—
4-*t*-Bu **8d**	A	4.49	−1.0	11.2	5.3	7.7
4-MeO **8e**	A	3.07	−2.5	10.0	5.1	—

[a] A = UB3LYP/6-311+G(2d,p)//UB3LYP/6-311+G(2d,p); B = UB3LYP/cc-pVTZ//UB3LYP/cc-pVTZ.

The UB3LYP/cc-pvtz computed energetics of the four competing reaction channels for the archetype radical **8a** are illustrated in Fig. 6. The *ortho*-cyclisation step to **11** is endothermic and has a comparatively high activation energy so does not compete in the accessible temperature range. A 1,4-phenyl shift would produce primary radical **3a** (analogous to **3** in Scheme 1). Although rearrangement to **3a** is only slightly endothermic, the required C–C bond fission in the *spiro*-intermediate **9a** has a high activation energy and so 1,4-phenyl shift

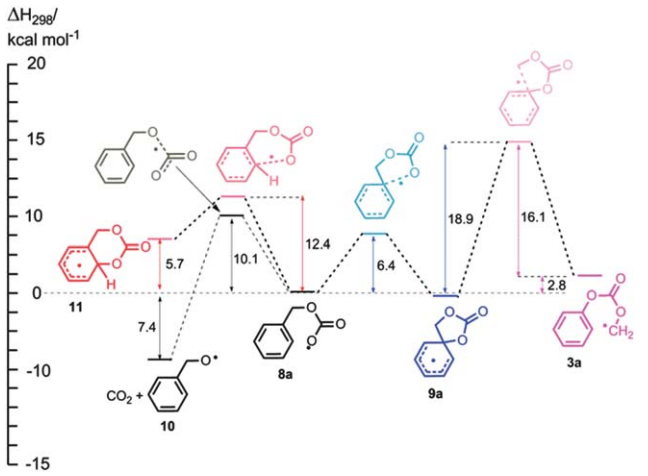

Fig. 6 UB3LYP/cc-pvtz computed reaction pathways for the benzyloxycarbonyloxyl radical **8a**.

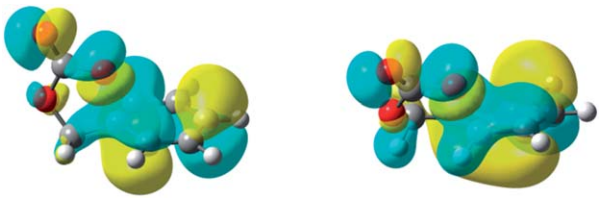

Fig. 7 DFT computed TS structures and SOMOs for *spiro*-(left, $\mathbf{TS}_{sp}$) and *ortho*-(right, $\mathbf{TS}_{or}$) cyclisations of radical **8a**.

cannot compete with C–O bond fission. β-Scission with loss of CO_2 is the most exothermic process but the activation energy of this step is comparatively high. This can partly be accounted for by the fact that the RO–C(O)O bond is strengthened by delocalization of the unpaired electron onto the RO moiety. The end result is that the dominant process at low temperatures is *spiro*-cyclisation, which is practically thermoneutral and has a lower activation energy than dissociation to CO_2. The latter process can only dominate at higher temperatures.

Why is *spiro*-cyclisation favoured over *ortho*-cyclisation for this range of benzyloxycarbonyloxyl radicals? The UB3LYP/6-311+D(2d,p) computed transition state structures, with their frontier SOMOs, are displayed in Fig. 7 for the two cyclisation modes and help to explain this.

The orbital containing the unpaired electron is a π-orbital *in the plane* of the ˙OC=O system (see $\mathbf{TS}_{sp}$). The geometry of the *spiro* approach to the ring is almost directly from above enabling this π-orbital to overlap very efficiently with the ring π-system. Thus the TS is early [r(O···C) = 1.929 Å, ∠C···O–C = 103.5°], the ring maintains much of its aromaticity, keeping the activation energy low. The geometry of *ortho* approach to the ring tilts the ˙OC=O π-orbital on its side such that overlap with the ring π-system is poorer (see $\mathbf{TS}_{or}$). The TS occurs later [r(O···C) = 1.885 Å, ∠C···O–C = 111.8°] with more disruption of the 6π ring system and hence a higher activation energy.

3 Conclusions

Benzyl oxime carbonates are easily made and handled and have long shelf lives. We have found them to be useful precursors for the photochemical generation of iminyl and alkoxycarbonyloxyl radicals. The latter radicals ring close exclusively by *spiro*-cyclisation onto the *ipso*-C-atom of the aromatic rings. The *spiro*-cyclohexadienyl radicals formed in this way were observable by EPR spectroscopy at temperatures below 270 K. In this way it was shown that β-scission of the alkoxycarbonyloxyls to CO_2 and BnO˙ radicals increasingly competes with *spiro*-cyclisation above about 210 K and becomes dominant above 270 K. Because of this the main products obtained from rt photolyses were derived from the BnO˙ and iminyl radicals.

A steady state kinetic equation was derived from the mechanism and enabled rate and Arrhenius parameters for the *spiro*-cyclisations to be estimated by the steady-state kinetic EPR method. Evidence from concentration measurements showed that the reverse *spiro*-ring opening was not important at the low temperatures of the EPR experiments. The *spiro*-rate constants were not very sensitive to substituents in the 4-positions of their aryl rings, although pentafluoro-substitution did reduce the rate. The *spiro*-rate constant for the archetype unsubstituted alkoxycarbonyloxyl **8a** was greater than that of the analogous *C*-centred radical, 4-phenylbutyl. This is consistent with the known high rates of alkoxycarbonyloxyl addition and abstraction reactions. As expected, however, the rate constant for *spiro*-cyclisation of **8a** was less than the rate constant for 5-*exo*-cyclisation of the archetype hex-5-enyl radical. Activation barriers of the *spiro*-cyclisations were computed by DFT to be about half those of the alternative *ortho*-cyclisations. The DFT computations also predicted lower barriers and faster rates for alkoxycarbonyloxyls with electron-releasing 4-substituents. However, in agreement with previous work, the B3LYP functional underestimated the reaction barriers. DFT found the *spiro*-cyclisations to be close to thermoneutral. Consideration of the TS structures suggested the preference for *spiro*- over *ortho*-cyclisation resulted from better overlap of the oxyl SOMO with the aromatic π-system during *spiro* closure.

Acknowledgements

We thank the EPSRC (grant EP/I003479/1) & EaStChem for funding, the EPSRC UK National Electron Paramagnetic Resonance Service at the University of Manchester and the EPSRC National Mass Spectrometry Service, Swansea. We are grateful to Dr Herbert Fruchtl for help with the computing.

Notes and references

1 (*a*) G. Pratsch and M. R. Heinrich, Radicals in Synthesis III, *Top. Curr. Chem.*, 2012, **320**, 33; (*b*) K. K. Laali and M. Shokouhimehr, *Curr. Org. Synth.*, 2009, **6**, 193.

2 See for example: (*a*) T. Cottin, C. Pyrkotis, C. I. Stathakis, I. Mavridis, I. A. Katsoulis, P. Anastasopoulou, G. Kythreoti, A. L. Zografos, V. R. Nahmias, A. Papakyriakou and D. Vourloumis, *ChemBioChem*, 2011, **12**, 71; (*b*) S. Beaumont, E. A. Ilardi, N. D. C. Tappin and A. Zakarian, *Eur. J. Org. Chem.*, 2010, 5743; (*c*) B. M. Trost and M. K. Brennan, *Synthesis*, 2009, 3003; (*d*) S. A. A. El Bialy, H. Braun and L. F. Tietze, *Synthesis*, 2004, 2249.

3 (*a*) D. H. Hey and A. R. Todd, *J. Chem. Soc. C*, 1967, 1518; (*b*) D. H. Hey, G. H. Jones and M. J. Perkins, *J. Chem. Soc. C*, 1971, 116; (*c*) D. H. Hey, G. H. Jones and M. J. Perkins, *J. Chem. Soc., Perkin Trans. 1*, 1972, 113.

4 (*a*) S. Guidott, R. Leardini, D. Nanni, P. Pareschi and G. Zanardi, *Tetrahedron Lett.*, 1995, **36**, 451; (*b*) D. Crich and J.-T. Hwang, *J. Org. Chem.*, 1998, **63**, 2765; (*c*) M. Koreeda, Y. Wang and L. Zhang, *Org. Lett.*, 2002, **4**, 3329; (*d*) A. K. Ganguly, C. H. Wang, T. M. Chan, Y. H. Ing and A. V. Buevich, *Tetrahedron Lett.*, 2004, **45**, 883; (*e*) F. G.-L. Turiso and D. P. Curran, *Org. Lett.*, 2005, **7**, 151; (*f*) K. C. Majumdar and S. Alam, *Org. Lett.*, 2006, **8**, 4059; (*g*) K. C. Majumdar, P. Debnath, A. K. Pal, S. K. Chattopadhyay and A. Biswas, *Can. J. Chem.*, 2007, **85**, 445; (*h*) C. V. Stevens, E. Van Meenen, K. G. R. Masschelein, Y. Eeckhout, W. Hooghe, B. D'Hondt,

V. N. Nemykin and V. V. Zhdankin, *Tetrahedron Lett.*, 2007, **48**, 7108; (*i*) T. Lanza, R. Leardini, M. Minozzi, D. Nanni, P. Spagnolo and G. Zanardi, *Angew. Chem., Int. Ed.*, 2008, **47**, 9439; (*j*) G. Rousseau, F. Robert and Y. Landais, *Chem.–Eur. J.*, 2009, **15**, 11160; (*k*) S. Van der Jeught, N. De Vos, K. Masschelein, I. Ghiviriga and C. V. Stevens, *Eur. J. Org. Chem.*, 2010, 5444; (*l*) Z. Tang, J. Mayrargue and M. Alami, *J. Heterocycl. Chem.*, 2011, **48**, 1238.

5 (*a*) W. R. Bowman, C. F. Bridge and P. Brookes, *J. Chem. Soc., Perkin Trans. 1*, 2000, 1; (*b*) H. Ohno, H. Iwasaki, T. Eguchi and T. Tanaka, *Chem. Commun.*, 2004, 2228.

6 (*a*) P. J. Parsons, M. Penverne and I. L. Pinto, *Synlett*, 1994, 721; (*b*) D. C. Harrowven, B. J. Sutton and S. Coulton, *Tetrahedron Lett.*, 2001, **42**, 9061; (*c*) C. Escolano and K. Jones, *Tetrahedron Lett.*, 2000, **41**, 8951.

7 J. K. Kochi and R. D. Gilliom, *J. Am. Chem. Soc.*, 1964, **86**, 5251.

8 (*a*) M. Julia, *Pure Appl. Chem.*, 1974, **40**, 553; (*b*) J. C. Chottard and M. Julia, *Tetrahedron*, 1972, **28**, 5615.

9 (*a*) J. A. Howard and K. U. Ingold, *Can. J. Chem.*, 1969, **47**, 3797; (*b*) C. Chatgilialoglu, K. U. Ingold and J. C. Scaiano, *J. Am. Chem. Soc.*, 1981, **103**, 7739.

10 A. L. J. Beckwith and K. U. Ingold, in *Rearrangements in Ground and Excited States*, ed. P. de Mayo, Academic Press, 1980, ch. 4, p. 161.

11 P. M. Brown, P. S. Dewar, A. R. Forrester and R. H. Thomson, *J. Chem. Soc., Perkin Trans. 1*, 1972, 2842.

12 (*a*) R. T. McBurney, A. M. Z. Slawin, L. A. Smart, Y. Yu and J. C. Walton, *Chem. Commun.*, 2011, **47**, 7974; (*b*) R. T. McBurney, A. D. Harper, A. M. Z. Slawin and J. C. Walton, *Chem. Sci.*, 2012, **3**, 3436.

13 D. J. Edge and J. K. Kochi, *J. Am. Chem. Soc.*, 1973, **95**, 2635.

14 Crystal data for **6d**: CCDC 923531, $C_{19}H_{21}NO_3$, $M = 311.38$, colourless prism, 0.120 × 0.030 × 0.030 mm, triclinic, $a = 6.229(3)$ Å, $b = 11.758(7)$ Å, $c = 12.009(7)$ Å, $c = 12.009(7)$ Å, $\alpha = 88.61(4)^\circ$, $\beta = 77.64(6)^\circ$, $\gamma = 83.80(4)^\circ$, $U = 854.1(8)$ Å^3, $T = 173$ K, space group *P*-1 (#2), $Z = 2$, 8939 reflections measured, 3049 unique, ($R_{int} = 0.1235$) which were used in all calculations. The final $wR(F_2)$ was 0.0964 (all data). Crystal data for **6f**: CCDC 923532, $C_{15}H_{12}FNO_3$, $M = 273.26$, colourless prism, 0.240 × 0.100 × 0.020 mm, monoclinic, $a = 14.698(2)$ Å, $b = 4.5311(5)$ Å, $c = 19.448(3)$ Å, $\beta = 97.309(4)^\circ$, $U = 1284.7(3)$ Å^3, $T = 173$ K, space group $P2_1/n$ (#14), $Z = 4$, 15766 reflections measured, 2261 unique, ($R_{int} = 0.0465$) which were used in all calculations. The final $wR(F_2)$ was 0.3223 (all data). Crystal data for **6g**: CCDC 923533, $C_{17}H_{17}NO_6S$, $M = 363.38$, colourless platelet, 0.100 × 0.100 × 0.010 mm, triclinic, $a = 5.707(7)$ Å, $b = 7.877(11)$ Å, $c = 18.99(3)$ Å, $\alpha = 98.61(6)^\circ$, $\beta = 91.40(8)^\circ$, $\gamma = 91.03(3)^\circ$, $U = 843(2)$ Å^3, $T = 173$ K, space group *P*-1 (#2), $Z = 2$, 11643 reflections measured, 2905 unique, ($R_{int} = 0.1733$) which were used in all calculations. The final $wR(F_2)$ was 0.4028 (all data). Crystal data for **7a**: CCDC 923534, $C_{15}H_8F_5NO_3$, $M = 345.23$, colourless platelet, 0.120 × 0.030 × 0.010 mm, monoclinic, $a = 7.89(3)$ Å, $b = 5.60(2)$ Å, $c = 16.51(6)$ Å, $\beta = 102.65(7)^\circ$, $U = 712(5)$ Å^3, $T = 173$ K, space group *P*21 (#4), $Z = 2$, 7300 reflections measured, 2479 unique, ($R_{int} = 0.1756$) which were used in all calculations. The final $wR(F_2)$ was 0.4300 (all data).

15 E. M. Scanlan, A. M. Z. Slawin and J. C. Walton, *Org. Biomol. Chem.*, 2004, **2**, 716.

16 F. Portela-Cubillo, J. Lymer, E. M. Scanlan, J. S. Scott and J. C. Walton, *Tetrahedron*, 2008, **64**, 11908.

17 A. R. Forrester and F. A. Neugebauer in *Landolt–Börnstein, Magnetic Properties of Free Radicals*, ed. H. Fischer and F. A. Neugebauer, Springer-Verlag, Berlin, 1979, vol. 9c1, pp. 115–121.

18 Note, however, that at 290 K decarboxylation of $C_6F_5CH_2OC(O)O^{\cdot}$ would be significant and therefore some of the H-abstraction may be due to $C_6F_5CH_2O^{\cdot}$ radicals.

19 Experiments could only be conducted down to 180 K with the 4-F-precursor **6f** because it was poorly soluble and crystallised out of the cyclopropane solvent.

20 See ESI for details of the derivation of eqn (1).†

21 (*a*) H.-H. Schuh and H. Fischer, *Helv. Chim. Acta*, 1978, **61**, 2130; (*b*) H.-H. Schuh and H. Fischer, *Int. J. Chem. Kinet.*, 1976, **8**, 341.

22 (*a*) B. Maillard and J. C. Walton, *J. Chem. Soc., Perkin Trans. 2*, 1985, 443; (*b*) A. F. Bella, L. V. Jackson and J. C. Walton, *J. Chem. Soc., Perkin Trans. 2*, 2002, 1839.

23 See: (*a*) A. L. J. Beckwith and S. Brumby, in *Landolt–Börnstein, Radical Reaction Rates in Liquids*, ed. H. Fischer, Springer Verlag, Berlin, 1994, vol. II18a, p. 171; (*b*) A. L. J. Beckwith, in *Landolt–Börnstein, Radical Reaction Rates in Liquids*, ed. H. Fischer, Springer Verlag, Berlin, 1984, vol. II13a, p. 252.

24 J. Chateauneuf, J. Lusztyk, B. Maillard and K. U. Ingold, *J. Am. Chem. Soc.*, 1988, **110**, 6727 and references cited therein.

25 The iminoxyl was almost certainly generated from trace impurities of the oxime in the starting material and was detected because of its persistence.

26 M. J. Frisch, *et al.*, Gaussian 09, Revision A.02, Gaussian, Inc., Wallingford CT, 2009, see ESI† for full citation.

27 J. P. Perdew, K. Burke and Y. Wang, *Phys. Rev. B: Condens. Matter*, 1996, **54**, 16533.

28 Y. Zhao and D. G. Truhlar, *Acc. Chem. Res.*, 2008, **41**, 157.

29 Y. Zhao, N. González-García and D. G. Truhlar, *J. Phys. Chem. A*, 2005, **109**, 2012.